U.S. DEPARTMENT OF COMMERCE
National Technical Information Service

PB-283 179

Studies of Dust Cake Formation and Structure in Fabric Filtration

Textile Research Inst, Princeton, N J

Prepared for

Industrial Environmental Research Lab, Research Triangle Park, N C

Jun 78

TECHNICAL REPORT DATA (Please read Instructions on the reverse before completing)		
1. REPORT NO. EPA-600/7-78-095	2.	3. RECIPIENT'S ACCESSION NO. PB283179
4. TITLE AND SUBTITLE Studies of Dust Cake Formation and Structure in Fabric Filtration		5. REPORT DATE June 1978 6. PERFORMING ORGANIZATION CODE
7. AUTHOR(S) Bernard Miller, George Lamb, Peter Costanza, Dan O'Meara, and Janet Dunbar		8. PERFORMING ORGANIZATION REPORT NO.
9. PERFORMING ORGANIZATION NAME AND ADDRESS Textile Research Institute P.O. Box 625 Princeton, New Jersey 08540		10. PROGRAM ELEMENT NO. EHE624 11. CONTRACT/GRANT NO. Grant R804926
12. SPONSORING AGENCY NAME AND ADDRESS EPA, Office of Research and Development Industrial Environmental Research Laboratory Research Triangle Park, NC 27711		13. TYPE OF REPORT AND PERIOD COVERED Final; 11/76-11/77 14. SPONSORING AGENCY CODE EPA/600/13

15. SUPPLEMENTARY NOTES IERL-RTP project officer is James H. Turner, Mail Drop 61, 919/541-2925.

16. ABSTRACT The report gives results of a study to identify cake characteristics affecting performance and, in turn, to relate the production of desirable cake properties to fabric structure and filtration conditions. (Earlier studies showed that differences in filtration performance produced by certain modifications of nonwoven filter fabrics are due largely to the development of different dust cake structures.) The amount of dust capture as a function of depth into the filter was measured using nonwovens formed in layers. Comparing trilobal cross-section filter fibers with round fibers, the largest advantages in capture efficiency due to trilobal fibers are in the upstream layers where the largest amounts of dust accumulate. Preliminary studies with composite layered filters also show that filtration performance is dominated by the upstream layer. Dust cake structure is influenced by fiber geometry, by the charge on the particles, and by any electric field on the filter. Theoretical calculations of single-fiber collection efficiencies support the experimental findings that capture of both charged and uncharged particles on fibers of any cross-sectional shape is more likely if an electric field is imposed perpendicular rather than parallel to the flow. As for fiber cross-sectional shape, capture should improve with increasing lobe number and depth.

17. KEY WORDS AND DOCUMENT ANALYSIS		
a. DESCRIPTORS	b. IDENTIFIERS/OPEN ENDED TERMS	c. COSATI Field/Group
Pollution Gas Filters Fabrics Nonwoven Fabrics Dust Caking Electric Fields	Pollution Control Stationary Sources Fabric Filters Particulate	13B 20C 13K 11E 11G 07A, 13H
18. DISTRIBUTION STATEMENT Unlimited	19. SECURITY CLASS (This Report) Unclassified 20. SECURITY CLASS (This page) Unclassified	21. NO. OF PAGES 49 22. PRICE A03 - A01

EPA Form 2220-1 (9-73)

United States
Environmental Protection
Agency

Industrial Environmental Research
Laboratory
Research Triangle Park NC 27711

EPA-600/7-78-095
June 1978

PB 283 179

EPA

Studies of Dust Cake Formation and Structure in Fabric Filtration

Interagency Energy/Environment R&D Program Report

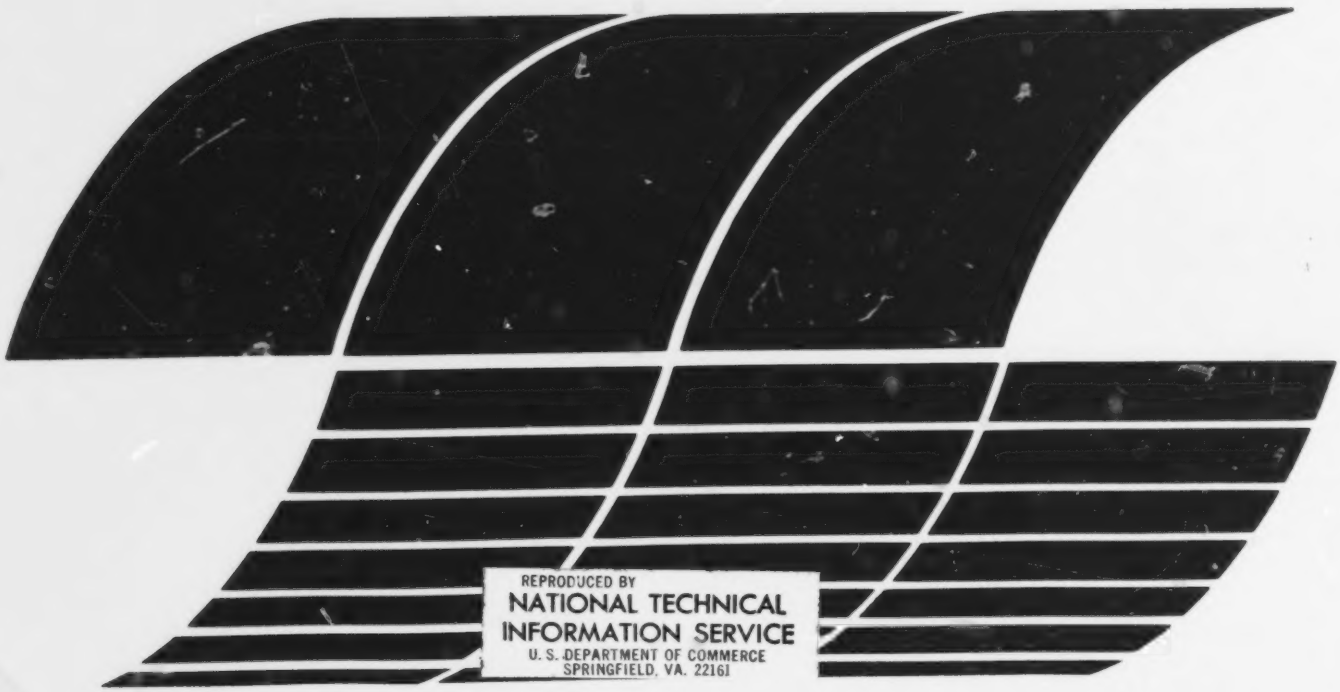

REPRODUCED BY
NATIONAL TECHNICAL
INFORMATION SERVICE
U. S. DEPARTMENT OF COMMERCE
SPRINGFIELD, VA. 22161

RESEARCH REPORTING SERIES

Research reports of the Office of Research and Development, U.S. Environmental Protection Agency, have been grouped into nine series. These nine broad categories were established to facilitate further development and application of environmental technology. Elimination of traditional grouping was consciously planned to foster technology transfer and a maximum interface in related fields. The nine series are:

1. Environmental Health Effects Research
2. Environmental Protection Technology
3. Ecological Research
4. Environmental Monitoring
5. Socioeconomic Environmental Studies
6. Scientific and Technical Assessment Reports (STAR)
7. Interagency Energy-Environment Research and Development
8. "Special" Reports
9. Miscellaneous Reports

This report has been assigned to the INTERAGENCY ENERGY-ENVIRONMENT RESEARCH AND DEVELOPMENT series. Reports in this series result from the effort funded under the 17-agency Federal Energy/Environment Research and Development Program. These studies relate to EPA's mission to protect the public health and welfare from adverse effects of pollutants associated with energy systems. The goal of the Program is to assure the rapid development of domestic energy supplies in an environmentally-compatible manner by providing the necessary environmental data and control technology. Investigations include analyses of the transport of energy-related pollutants and their health and ecological effects; assessments of, and development of, control technologies for energy systems; and integrated assessments of a wide range of energy-related environmental issues.

EPA REVIEW NOTICE

This report has been reviewed by the participating Federal Agencies, and approved for publication. Approval does not signify that the contents necessarily reflect the views and policies of the Government, nor does mention of trade names or commercial products constitute endorsement or recommendation for use.

This document is available to the public through the National Technical Information Service, Springfield, Virginia 22161.

EPA-600/7-78-095
June 1978

Studies of Dust Cake Formation and Structure in Fabric Filtration

by

Bernard Miller, George Lamb, Peter Costanza,
Dan O'Meara, and Janet Dunbar

Textile Research Institute
P.O. Box 625
Princeton, New Jersey 08540

Grant No. R804926
Program Element No. EHE624

EPA Project Officer: James H. Turner

Industrial Environmental Research Laboratory
Office of Energy, Minerals, and Industry
Research Triangle Park, NC 27711

Prepared for

U.S. ENVIRONMENTAL PROTECTION AGENCY
Office of Research and Development
Washington, DC 20460

ABSTRACT

Earlier studies have shown that differences in filtration performance produced by certain modifications of nonwoven filter fabrics are largely due to the development of different dust cake structures. The chief objectives of the current program are to identify those cake characteristics affecting performance and in turn to relate the production of desirable cake properties to fabric structure and filtration conditions.

One experimental approach has involved microscopical examination of flyash deposits on nonwoven fabrics. In a more quantitative approach, the amount of dust capture as a function of depth into the filter was measured using nonwovens formed in layers. When filters made of fibers with trilobal cross sections are compared with those made of round fibers, the largest advantages in capture efficiency due to trilobal fibers occur in the upstream layers where the largest amounts of dust accumulate. Preliminary studies with composite layered filters also show that filtration performance is dominated by the upstream layer. For example, a filter of mostly round fibers with only a narrow upstream layer of trilobal fibers has the higher efficiency and lower pressure drop of an all-trilobal filter.

Dust cake structure is influenced not only by fiber geometry but also by the charge on the particles and by any electric field on the filter. Neutralizing the naturally charged flyash particles results in a more compact, less porous cake and in increased pressure drop. When the particles are precharged, they appear to collect closer to the surface and not to collapse into pores as readily, resulting in increased efficiency and lower pressure drop. An electric field set up across the filter perpendicular to the air flow can also produce higher efficiency and reduced pressure drop. When incoming particles are charged, either naturally or by precharging, more dust is deposited near the electrodes of opposite charge, creating regions of differing resistance to air flow, which probably account for some of the observed reduction in pressure drop.

Theoretical calculations of single-fiber collection efficiencies support the experimental findings that capture of both charged and uncharged particles on fibers of any cross-sectional shape is more likely if an electric field is imposed perpendicular rather than parallel to the flow. In regard to fiber cross-sectional shape, capture should improve with increasing number of lobes and with the depth of the lobes.

This report is submitted in fulfillment of Grant No. R804926-1 by Textile Research Institute under the sponsorship of the U. S. Environmental Protection Agency. This report covers a period from December 20, 1976 to December 19, 1977, and work was completed in December 1977.

CONTENTS

	Page
Abstract	ii
Figures	iv
Tables	vi
Acknowledgments	vii
I. INTRODUCTION	1
II. EFFECT OF FIBER GEOMETRY ON DUST CAKE FORMATION	2
A. TRILOBAL AND ROUND CROSS-SECTIONAL SHAPE	2
1. Introduction	2
2. Photographic Studies	2
3. Measurements of Cake Density as a Function of Depth into Fabric	5
4. Composite Filters	9
5. Observations on Fiber Arrays	10
B. ROUGH AND SMOOTH FIBER SURFACES	11
C. EFFECT OF PARTICLE CHARGE	13
1. Neutralized Aerosols	13
2. Effect of Particle Precharging	16
III. STUDIES OF CAPTURE IN ELECTRIC FIELDS	19
A. THEORETICAL STUDIES	19
1. Effect of Field Orientation	19
2. Fibers With Lobed Cross Sections	22
B. EFFECT OF ELECTRIC FIELD ON CAKE STRUCTURE	31
1. Introduction	31
2. Experimental Results	31
3. Conclusions	36
IV. REFERENCES	38

FIGURES

Number		Page
1	Technique for formation of dust cake directly on SEM specimen	3
2	Loss of particles apparently due to bombardment by electron beam	4
3	Scanning electron micrographs comparing dust deposits formed on round and trilobal fiber filters at a dust loading of 2 mg/cm^2. 500X	4
4	Filtration performance of layered bonded nonwovens made of round and trilobal fibers. Face velocity 12 fpm	6
5	Filtration performance of another pair of layered nonwovens made of round and trilobal fibers	7
6	Filtration performance of a third pair of layered nonwovens made of round and trilobal fibers. Note: These fabrics are almost twice as dense as those of Figures 4 and 5	8
7	Scanning electron micrographs comparinf dust cakes formed on trilobal and round fiber filters (50X), and smooth fiber filters (100X) by an untreated flyash aerosol	12
8	Scanning electron micrographs comparing dust cakes formed on trilobal and round fiber filters (200X), and rough and smooth fiber filters (100X) by a neutralized flyash aerosol	14
9	Pressure drop developed by increasing dust cake deposits of untreated and neutralized flyash aerosols on trilobal and round fiber filters	15
10	Efficiency of trilobal and round fiber filters with increasing deposits of untreated and neutralized flyash	15
11	Pressure drop developed by increasing dust cake deposits of untreated and neutralized flyash aerosols on rough and smooth fiber filters	17
12	Efficiency of rough and smooth surface fiber filters with increasing deposits of untreated and neutralized flyash	17
13	The two limiting particle trajectories for a round fiber of radius r_c	20
14	Enhancement e of collection efficiency by a field perpendicular to the flow for charged particles as a function of $\|G\| = qE_oB/V_o$	20

Figures (con.)

Number		Page
15	Fiber cross sections for selected values of m (number of fiber lobes), c (orientation of fiber to air flow), and size of lobes	22
16	Particle trajectories near a bilobal fiber. Field parallel to air flow, a = 0.5, and F = 1.0	23
17	Particulate trajectories near a trilobal fiber. Field parallel to air flow, a = 0.5, and F = 1.0	23
18	Comparison of collection efficiencies for bilobal and trilobal fibers at different orientations of fiber to electric field	24
19	Comparison of the effective diameters of multilobal fibers (for charged particles)	28
20	Effective fiber diameter vs. number of lobes (for charged particles)	28
21	Effect of fiber orientation on the effective diameter of a bilobal fiber (for charged particles)	29
22	Diagram of tube for precharging flyash aerosol (negative precharging arrangement)	30
23	Positively precharged particles deposited on filter in absence of applied field across filter	33
24	Neutralized particles deposited on filter in absence of applied field across filter	33
25	Naturally charged particles deposited on filter in absence of applied field across filter	33
26	Naturally charged particles deposited on filter with 2 kV/cm across filter	34
27	Positively precharged particles deposited on filter with 2 kV/cm across filter	34
28	Negatively precharged particles deposited on filter with 2 kV/cm across filter	35
29	Neutralized particles deposited on filter with 2 kV/cm across filter	35
30	Two sets of two electrodes with 2-kV/cm potential gradient using naturally charged particles	35
31	Electrical analogy of unequal parallel resistances	37

TABLES

Number		Page
1	Performance of Composite Fabrics in Filtering a Fly-ash Aerosol of 7 g/m^3 After 24 Cycles of Conditioning	10
2	Cake Resistance and Efficiency of Round and Trilobal Fiber Filters when Filtering Aerosols Charged to Various Levels	18
3	Comparison of Collection Efficiencies for Uncharged Particles Acted on by Electric Fields Parallel and Perpendicular to the Flow Direction	21
4	Collection Efficiencies for Uncharged Particles on 1-, 2-, and 3-lobe Fibers in Electric Fields	24

ACKNOWLEDGMENTS

The authors would like to express their appreciation to Dr. James H. Turner of the Environmental Protection Agency for his advice and encouragement throughout the period of this research. They would also like to thank Mr. Harold W. Lambert and Mr. Harry Buvel of TRI for their invaluable work on apparatus, Mr. John P. Hession for his assistance with microscopy, and Dr. Harriet G. Heilweil for her help with reports.

SECTION I

INTRODUCTION

The main object of this work is to find explanations for observed changes in filtration performance that result from certain modifications of conventional fabric filtration technology. One such modification is the use of fibers having different geometric properties (cross-sectional shape, surface roughness, crimp, etc.) from those fibers generally used in filter fabrics. Another is the application of electric fields to the fabrics. A third, the use of creped fabrics. In each case, some of the improvements in performance, which have taken the form of increased capture efficiency, reduced pressure drop, or both, appear to be coincident with changes in dust cake characteristics. Therefore, one aspect of the present work is the identification of certain features of the dust cake or of the fabric-dust cake system, which may explain the observed changes in performance. A second goal is to use this information as a basis for the design of improved filter fabrics.

SECTION II

EFFECT OF FIBER GEOMETRY ON DUST CAKE FORMATION

A. TRILOBAL AND ROUND CROSS-SECTIONAL SHAPE

1. Introduction

A previous study [1] of the differences in capture efficiency between nonwoven filters made of fibers of round as opposed to trilobal cross section attempted to explain the results as a consequence of dissimilar interfiber distances. In two fabrics having the same packing density, if the fibers have equal linear density but different cross-sectional shapes, the average center-to-center interfiber distance will be the same, but the effective spacing between fibers will be different and slightly smaller for trilobal than for round fibers. It may be argued that the smaller interfiber gaps in trilobal fiber fabrics would give rise to more readily formed and more stable dust bridges and in this way to higher collection efficiencies. The dependence of collection efficiency on round-fiber diameter at constant packing density has been measured, however, and from this the dependence on the interfiber gap. The change in diameter of a round fiber that would produce the same reduction in interfiber gap as a trilobal fiber of the same linear density was calculated. The increase in efficiency corresponding to this smaller interfiber gap with round fibers is only half of the increase in efficiency obtained experimentally from the same decrease in interfiber gap due to change from round to trilobal shape. It is likely, therefore, that trilobal fibers enhance capture, not only because of reduced interfiber gap, but also by some other mechanism. It is notable also that, in general, trilobal fibers do not cause increased pressure drop.

2. Photographic Studies

An initial effort of the present program consisted of a microscopical study of dust formations on nonwoven filters, using at first a scanning electron microscope (SEM) and later, a binocular light microscope. The study was begun with the development of a technique for preparing a filter sample suitable for SEM examination. A 1-in. diameter disc of filter fabric was glued to an annular aluminum stub of 1-in. o.d. and 0.75-in. i.d. This stub could be inserted directly into the SEM sample holder. The stub was then glued to the center of a patch filter specimen of the same fabric, in which a 0.75-in. hole had been cut. The arrangement is shown in Figure 1. In this way dust could be deposited on the test specimen using the TRI patch filter apparatus with only minor disturbance of the flow pattern. The stub was then pulled off the patch filter for SEM examination.

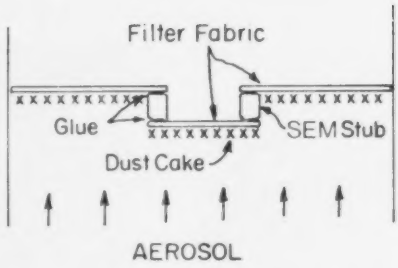

Figure 1. Technique for formation of dust cake directly on SEM specimen.

The microscopical study was aimed at identifying features of the dust deposit which would explain the better performance of trilobal fibers over round. Two levels of dust loading were used: 1) $\sim$2 mg/cm^2, a low cake mass to observe incipient bridging, and 2) $\sim$15 mg/cm^2, a normal cake mass encountered in practice.

With a light dust loading, problems were caused by the interaction of the SEM and the incipient dust cake. Consecutive photographs taken of the same area of filter with dust deposited on it showed fewer particles on later photographs. It appeared that the electron beam bombardment knocked particles off the sample. This illustrates the fragility of the structures to be studied and also places in doubt the suitability of scanning electron microscopy as a method for this type of study. Figure 2 shows an example of such a sequence of photographs. It can be seen that the lettered particles are missing in Figure 2b which was taken a short time after Figure 2a. In Figure 3 are examples of views of light dust deposits on round (a) and trilobal (b) fiber filter substrates which illustrate the difficulty of identifying any features that could be correlated with differences in performance.

When a normal cake mass was deposited on the filters, lower magnification (50X) provided some indication that trilobal fibers form a filter substrate for a more uniform cake with fewer voids and asperities (Fig. 7a). This greater uniformity can apparently be associated with higher capture efficiency and with greater ease of cleaning resulting in lower pressure drop. However, since the interface between the dust cake and the substrate could not be seen, an explanation for the greater uniformity cannot be offered. A top view under the SEM is not acceptable, and some means of viewing the cake/fabric interface must be developed before the effect of fiber cross section can be optimized.

In the proposal submitted originally, several methods for microscopical examination of dust cakes were listed, each of which was meant to be tried in turn. The methods were themselves not well established but were implicitly expected to require a certain amount

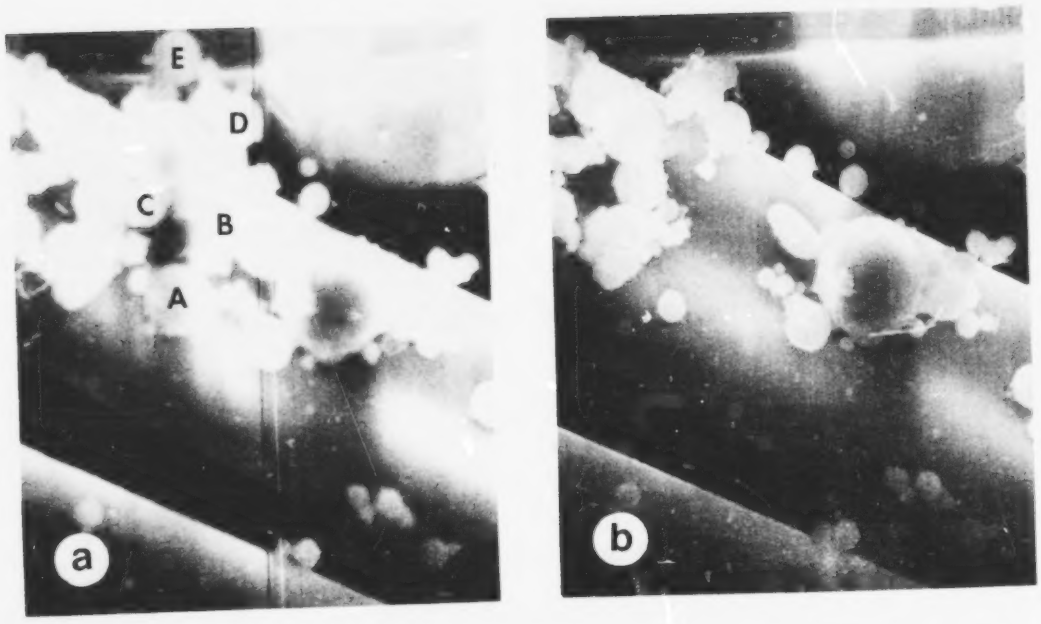

Figure 2. Loss of particles apparently due to bombardment by electron beam. Particles A - E are missing from photograph (b) taken a short time after (a).

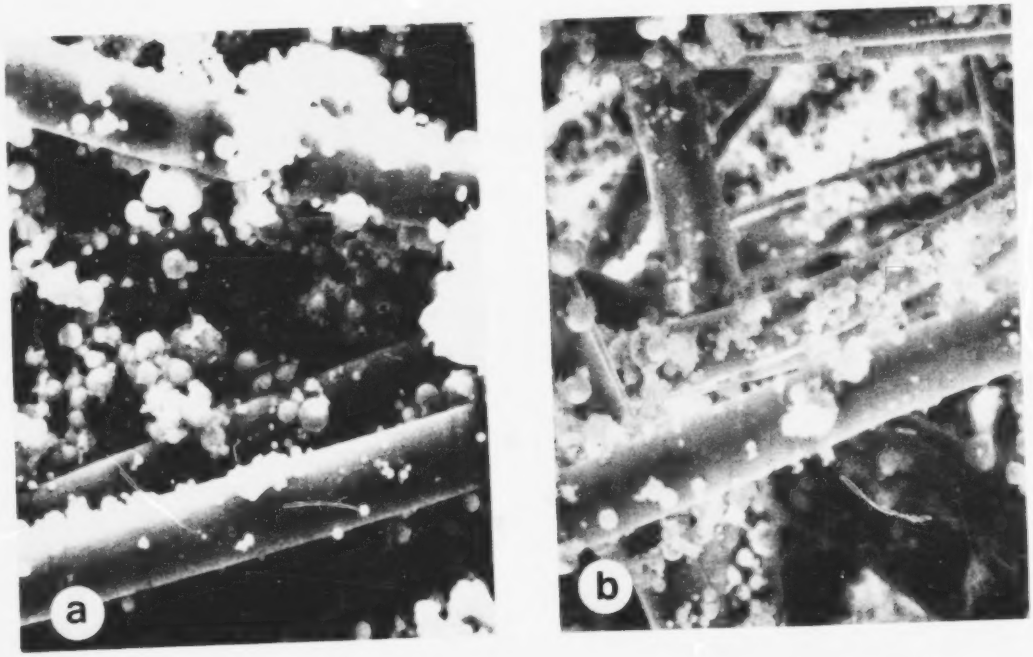

Figure 3. Scanning electron micrographs comparing dust deposits formed on (a) round and (b) trilobal fiber filters at a dust loading of 2 mg/cm^2. 500X.

of development before they proved suitable for the present purpose. They included various techniques for embedding and sectioning the fabric/cake combination, as well as other techniques for exposing a sectional view of the dust cake by removing adjacent areas of the cake using suction techniques. However, the inconclusive outcome of the first stage of this work made it desirable to investigate other techniques which might meet with greater success. Therefore the emphasis was shifted towards what was felt to be a more quantitative analysis, namely the measurement of cake density with depth into the filter.

3. Measurements of Cake Density as a Function of Depth into Fabric

The word cake tends to mislead because it conveys the image of a sharp boundary between the deposited dust layer and the fabric. This is not in fact true, since dust and fabric interpenetrate to an extent which ultimately determines both efficiency and pressure drop characteristics.

Card webs were made from round and trilobal 3-denier polyester (PET) fibers, each containing a minor amount of binder fiber. Pieces of card web of different thickness were compressed under heat to form a large number of thin fabric patches. These were trimmed and weighed. Layered fabrics were then formed from patches selected so that corresponding layers in the round and trilobal fabrics would be close in weight. By controlling the forming pressure, densities of the fabrics were made as uniform as possible.

After filtering a flyash aerosol through these layered fabrics, the layers were peeled apart and weighed. The results of three such experiments, each comparing a round and a trilobal filter, are shown in Figures 4, 5, and 6. In each case, the penetration (1-E) and the single fiber efficiency η are plotted vs. the depth into the filter ("a" and "b" plots), and the single fiber efficiency is plotted vs. the local aerosol concentration ("c" plots).

As seen in Figures 4c, 5c, and 6c, the collection efficiency is rather sensitive to both aerosol concentration and packing density α, and consequently the "a" plots do not show a consistent trend, the penetration for trilobal fibers being less than for round in Figures 4a and 6a but more in Figure 5a. Greater consistency is seen in the "b" figures, which normalize for packing density by plotting the single fiber efficiency η. This quantity is calculated from the relationship

$$\eta = \frac{\ell n(1-E)}{\Delta x} \cdot \frac{\pi R(1-\alpha)}{2\alpha}, \qquad (1)$$

where (1-E) is the penetration, Δx the thickness of the layer, R the fiber radius, and α the packing density. The penetration (1-E) for each layer used in this calculation is the value given in the "a" plot, divided by the value for the previous upstream layer. The "b" plots, being normalized for packing density, give a truer comparison of the two types of fabric, and indicate a tendency for the efficiency to be higher for trilobal fibers in the upstream layer, but to be equal in the downstream layers. This is brought out slightly better in the "c" figures, which eliminate the effect of concentration by plotting

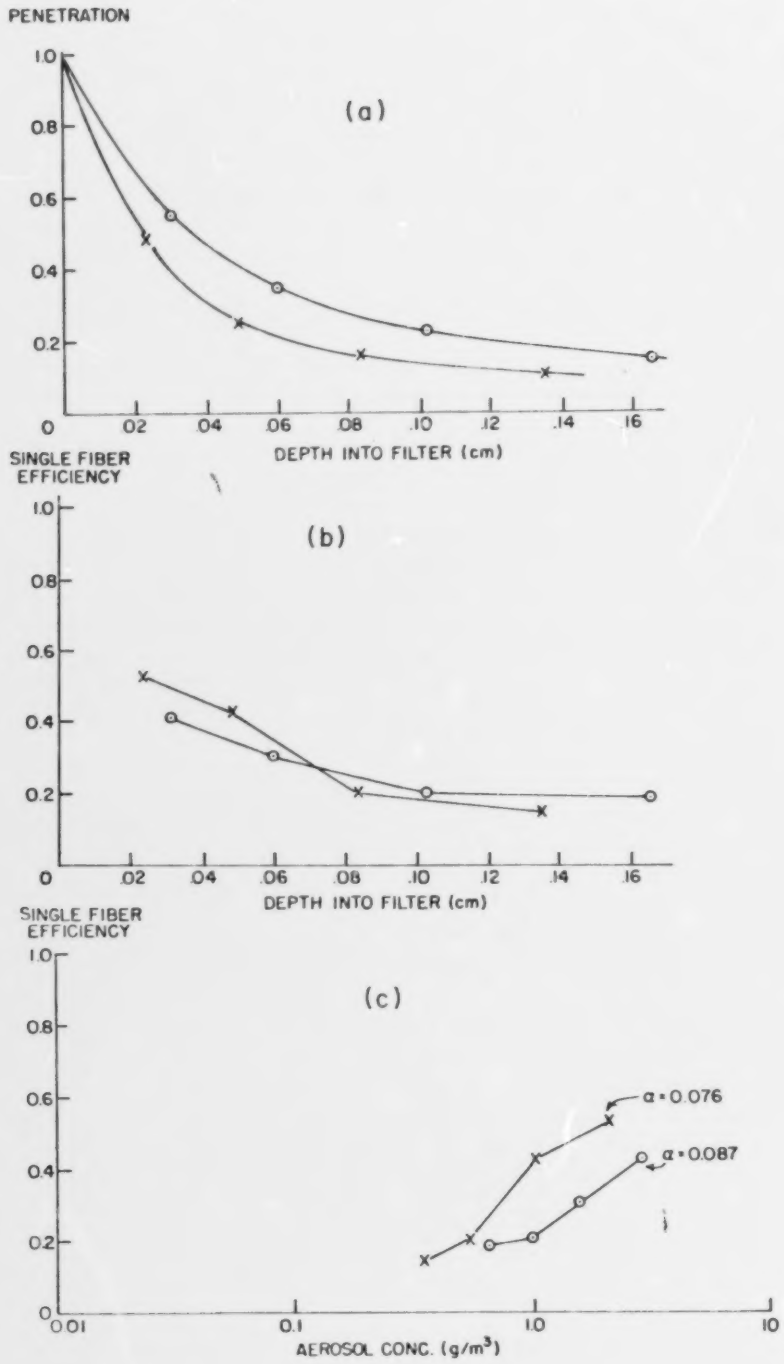

Figure 4. Filtration performance of layered bonded (15% vinyon) nonwovens made of round (o) and trilobal (x) fibers. Face velocity 12 fpm. Points plotted at center of layer thickness.

(a) Penetration vs. depth into filter.
(b) Single fiber efficiency vs. depth into filter.
(c) Single fiber efficiency vs. aerosol concentration.

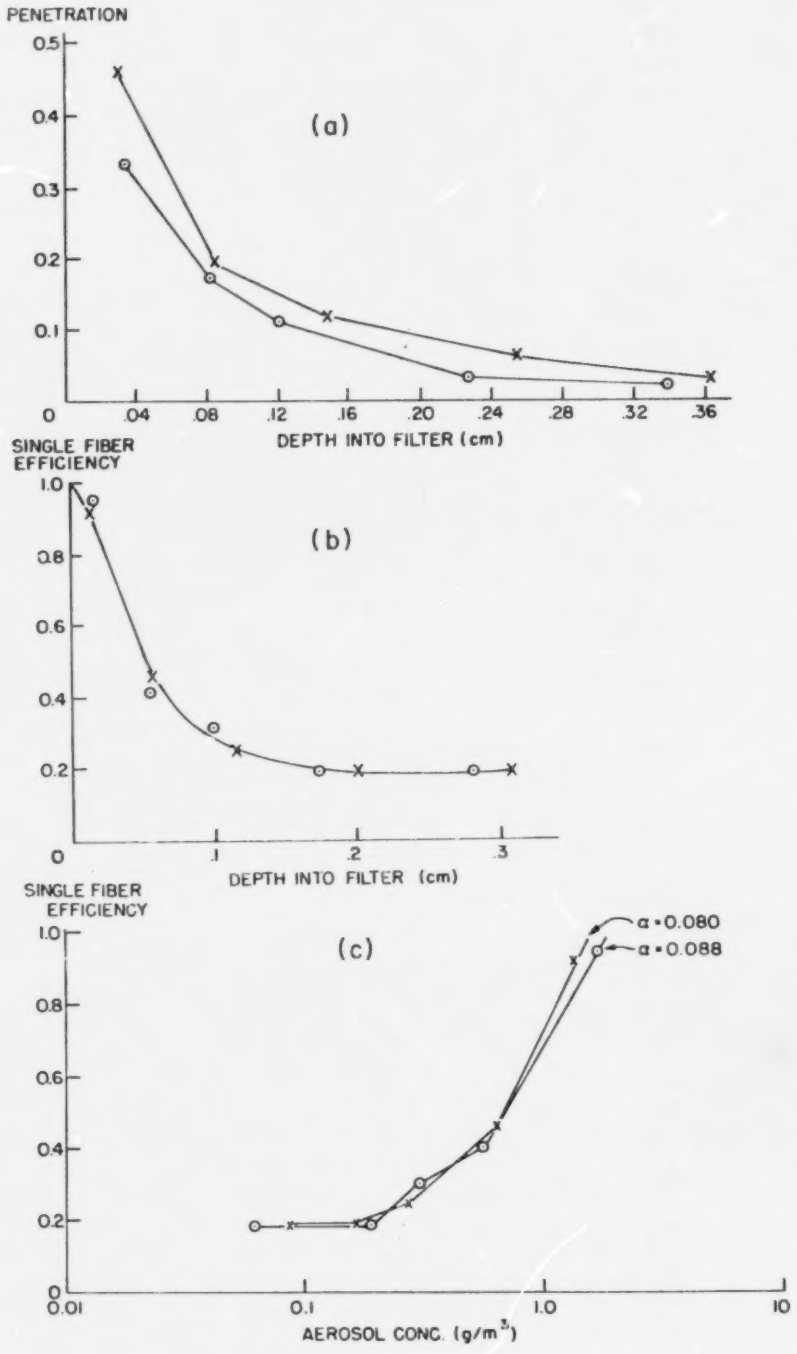

Figure 5. Filtration performance of another pair of layered nonwovens made of round (•) and trilobal (x) fibers.

(a) Penetration vs. depth into filter.
(b) Single fiber efficiency vs. depth into filter.
(c) Single fiber efficiency vs. aerosol concentration.

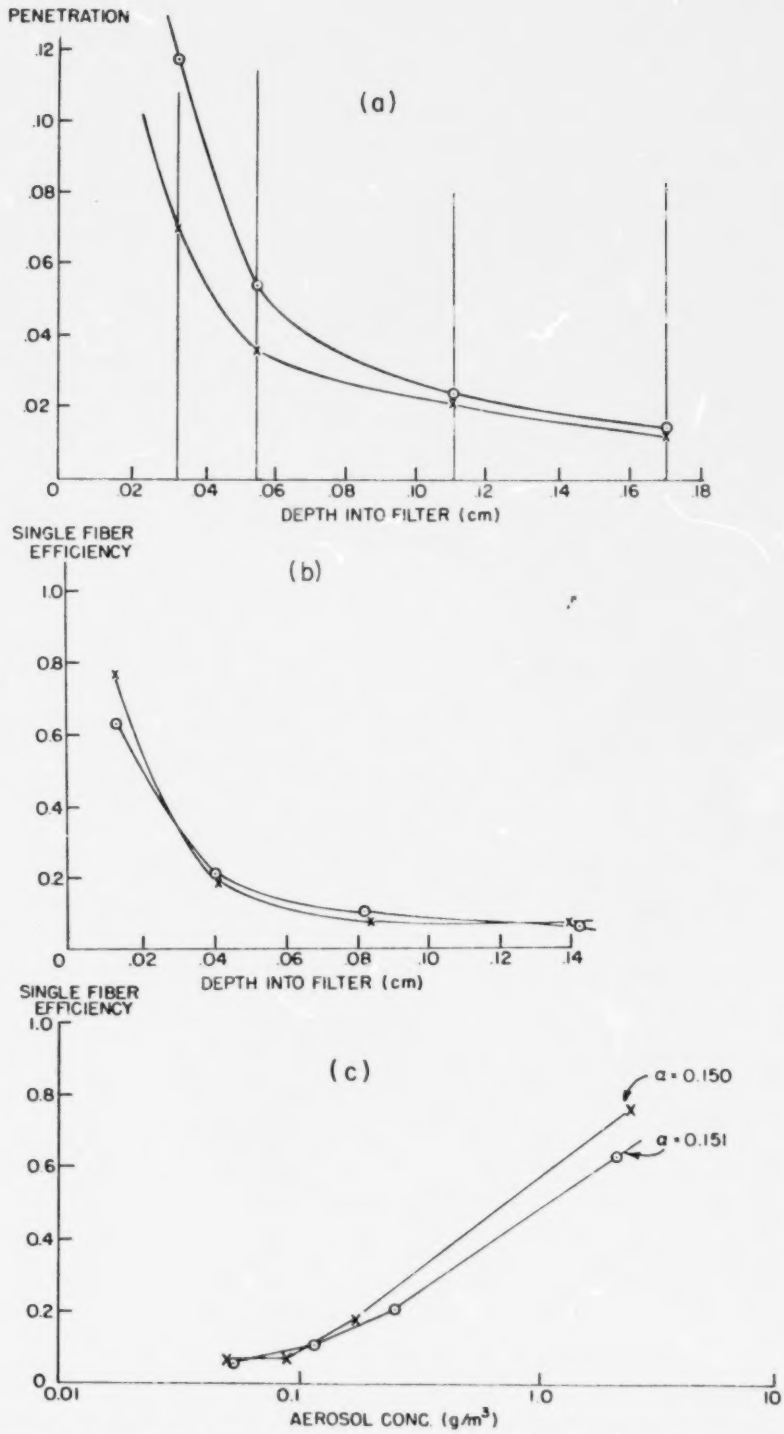

Figure 6. Filtration performance of a third pair of layered nonwovens made of round (∘) and trilobal (x) fibers. Note: These fabrics are almost twice as dense as those of Figures 4 and 5.

(a) Penetration vs. depth into filter.
(b) Single fiber efficiency vs. depth into filter.
(c) Single fiber efficiency vs. aerosol concentration.

single fiber efficiency vs. concentration. The efficiency rises rapidly with concentration, clearly due to the accumulation of dust cake, which occurs more rapidly on the upstream layers, rather than to any change in the capture mechanism. In these "c" plots the efficiency is greater for trilobal fibers than for round, but only for the layers on which a dust cake has collected. At lower concentrations (i.e., the downstream layers) efficiencies are equal. This finding is consistent with previous observations of differences in performance between fabrics made with round and trilobal fibers only when filtering aerosols of sufficient concentration to deposit a cake. With very dilute aerosols, no differences were seen.

In explaining the superior performance of one type of fiber over the other, these findings do not appear to lead to very simple models, since the downstream layers do not exhibit the better single fiber efficiency predicted for lobed fibers by theoretical considerations. However, some mechanism must be acting to cause the differences in efficiency in the upstream layers.

4. Composite Filters

The results in the previous section prompted initial studies involving composite filters. These would be filters made of more than one fiber type, with the different fibers arranged in layers and/or in blends in such a way as to gain the advantage given by each type of fiber.

The first study involved a set of fabrics made of layers as shown in Table 1. Two of the fabrics were made up of only either trilobal or round fibers, the other two had an upstream layer of trilobal fibers in one case and of round fibers in the other, the remainder being of the other fiber. The upstream layers amounted to one sixth of the filter mass. The filters were all conditioned for 24 cycles with a flyash aerosol of 7 g/m^3. Table 1 gives the results. It is clear that the behavior of the filters is dominated by the nature of the upstream layer, with the downstream layers playing a minor role. These results agree with the data (e.g., Fig. 6b) showing that the efficiencies of downstream layers are equal for round and trilobal fibers. They also support data obtained previously with filter bags, which showed that trilobal bags gave higher efficiency and lower pressure drop than round ones [1].

The reason for the lower pressure drop exhibited by the filters with trilobal upstream layers is not readily apparent. The lower pressure drop is observed with trilobal fabric even though the cake mass is higher in the upstream layer of that fabric. It follows that the cake density must be less. This however could not be confirmed by microscopical observation, neither could any special features of the cakes be discerned that would explain the formation of a less dense cake.

TABLE 1. PERFORMANCE OF COMPOSITE FABRICS IN FILTERING A FLYASH AEROSOL OF 7 g/m^3 AFTER 24 CYCLES OF CONDITIONING

Upstream layer	Downstream layer	C_o (mg/m^3)	ΔP (mm H_2O)
Trilobal (1.2 oz/yd^2)	Round (6.2 oz/yd^2)	3.44	69.7
All trilobal (7.4 oz/yd^2)		3.33	68.2
Round (1.2 oz/yd^2)	Trilobal (6.2 oz/yd^2)	6.67	76.8
All round (7.4 oz/yd^2)		6.78	78.9

Filter thickness: ∿1.8 mm
Surface layer thickness: ∿0.3 mm

In a practical application, greater efficiency might be obtained by combining an upstream layer that is efficient at the inlet concentration with downstream layers that are more efficient at the lower concentrations found deeper in the filter; as for example, by utilizing larger numbers of finer fibers (at the same packing density) for some of the downstream layers.

5. Observations on Fiber Arrays

The results of the preceding section indicate that efficiency is controlled by the nature of the fibers (trilobal vs. round) in the upstream layer but not in the downstream layers. This suggests that in the upstream layer, even though the efficiency of the bare fibers may be equal, the dust accumulates in such a manner as to facilitate further collection and the more rapidly formed cake promotes greater efficiency. Since microscopical examination of dust cakes on random nonwovens revealed no features that would confirm such an hypothesis, some time was devoted to attempts to build incipient dust cakes on regular fiber arrays that might, by occurring in a more regular fasion, be easier to observe.

The arrays were made by hand and consisted of sets of parallel fibers separated by a distance of 3 fiber diameters. The arrays were formed on aluminum annuli which had been made to fit a scanning electron microscope stage. On each annulus, arrays of trilobal and round fibers were formed side by side in order to make direct comparisons of the features of the deposited dust.

Three kinds of arrays were made, of increasing complexity. The first consisted of a row of eight parallel fibers. The second consisted of two layers of eight-fiber rows, the rows oriented perpendicular to each other. The third consisted of three eight-fiber sets, alternating in orientation, such that there were three layers of fibers at the intersections.

In each case, the annulus was placed in a duct and exposed for five minutes to a 12-fpm stream of flyash aerosol. The annulus was then examined under a binocular microscope, which gave adequate magnification for rapid inspection of the dust deposits. It was planned to use scanning electron microscopy for closer study and for recording any structure of interest. However, no such structures were seen. Capture on single rows of fibers revealed a great deal of nonuniformity between fibers of the same kind and even from place to place on one fiber. This nonuniform behavior made impossible meaningful comparison of capture between the two kinds of fiber. In any case, the dust buildup that was the most important feature sought was not observed. The overlapping rows of fibers, which were expected to give more stable accumulations, did not do so. In all cases some capture occurred, but the proximity of adjacent fibers did not affect capture on any individual one. The uneven deposition on individual fibers was assumed to be due to areas of electrostatic charge.

This study of model fabrics will continue with some of the following modifications:

1) Metallizing of the fibers to eliminate uncontrolled static surface charges, and neutralization of the aerosol particles. This will be done to ensure a measure of control on electrostatic effects, which otherwise occur in a random fashion.

2) Changes in the array construction to promote the formation of dust cakes. Although the fiber-fiber spacings, equal to three fiber diameters, are about equal to average interfiber spacings in a nonwoven fabric, the parallel arrangement in the model fabrics may require smaller spacings in order to form a stable cake.

3) Cake formation in the presence of electric fields. The effects which are to be studied in these conditions are discussed in a following section (III).

B. ROUGH AND SMOOTH FIBER SURFACES

Although present studies of fiber geometry effects on dust cake formation have concentrated on round and trilobal fiber cross sections, some time has also been devoted to differences due to rough and smooth fiber substrates. In these studies the rough fibers contained a greater percentage of TiO_2 (2.0%) than the smooth fibers (0.1%), so that a slightly greater number of surface asperities were present in the rough fibers. Previous studies indicated that rough fiber substrates produce slightly greater filter efficiencies than round, but no significant differences were seen in pressure drop after conditioning [1].

Studies of dust cake formation on rough- and smooth-fiber needled nonwoven filters thus far mainly consist of microscopical examination. Studies of layered or composite filters have not yet been conducted. However, in the next section the effect of particle charge is considered for rough and smooth fiber filters as well as for trilobal and round.

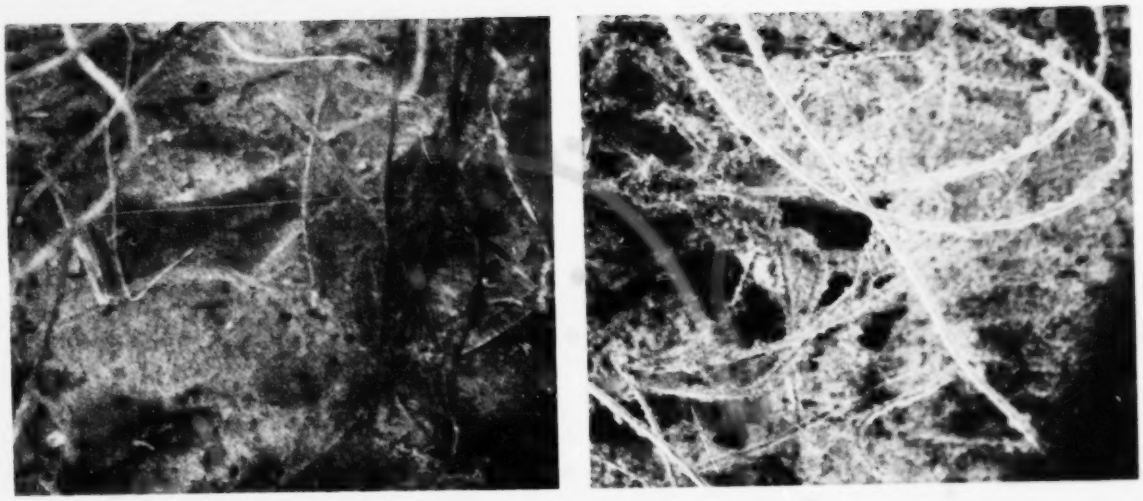

a

Trilobal

Round

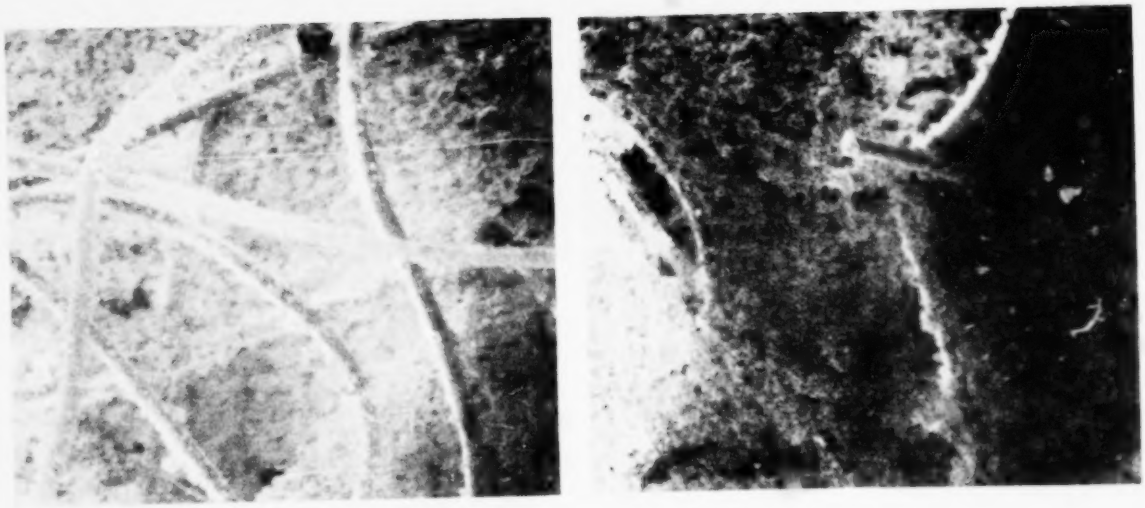

b

Rough

Smooth

Figure 7. Scanning electron micrographs comparing dust cakes formed on (a) trilobal and round fiber filters (50X), and (b) rough and smooth fiber filters (100X) by an untreated flyash aerosol.

Microscopical examination followed the same procedure discussed in the previous section. High magnifications of light dust loadings revealed no differences. SEM micrographs of heavier dust loadings such as the ones shown in Figure 7b also do not reveal any differences in cake structure formed on the two types of fabric. At 50X, unlike the comparison between trilobal and round fiber substrates, no differences in cake uniformity can be seen. This observation agrees with the results in Figures 11 and 12, which indicate no differences in pressure drop or efficiency for the two fabrics on the first cycle. Since earlier studies indicated slightly greater efficiencies for the rough fiber fabric after conditioning, further examination of cakes formed after many cycles will be conducted.

C. EFFECT OF PARTICLE CHARGE

1. Neutralized Aerosols

Further studies of trilobal vs. round and of rough vs. smooth fiber filters were conducted using the same needled fabrics. The objective was to observe the differences in performance as a function of cake mass and as a function of particle charge. In this case the flyash aerosol was passed through a charge neutralizer before it went on to the filter.

SEM photographs of the dust cakes obtained with the neutralized aerosol are shown in Figure 8. Those formed on trilobal fabrics appear to be more uniform than those on round fabrics (Fig. 8a). The dust cakes formed on rough and smooth fiber fabrics, on the other hand, appeared to be very much alike (Fig. 8b). The latter observation is not unexpected in view of the absence of distinguishing features in dust cakes formed on rough and smooth fiber fabrics with untreated aerosol, i.e., with aerosol having more charged particles. If an important effect of lobes or surface asperities is to produce locally intensified electric fields due to naturally occurring electric charges on the fibers, the removal of the particle charges will reduce any difference between the cake formed on rough and smooth fibers.

Results of pressure drop and efficiency measurements with neutralized aerosol are given in Figures 9 through 12. Each data point was obtained with the filter freshly cleaned by vacuum cleaning. In Figure 9 it can be seen that for unneutralized particles pressure drop increases with cake mass equally for trilobal and for round fiber filters until an abnormally high cake mass is reached ($\sim$30 mg/cm^2). The "trilobal" curve then increases rapidly, whereas the "round" curve remains approximately linear. The trilobal structure with its smaller interfiber spacings will therefore eventually cause pressure drop to rise more rapidly than the round structure. However, at the higher cake mass efficiency continues to remain higher for trilobal than for round fiber filters (Fig. 10).

In Figure 9 it can be seen that the same ΔP relationship between trilobal and round holds for neutralized particles, although the curves are shifted in the direction of greater ΔP at lower cake mass. It appears that the presence of uncharged particles results in more

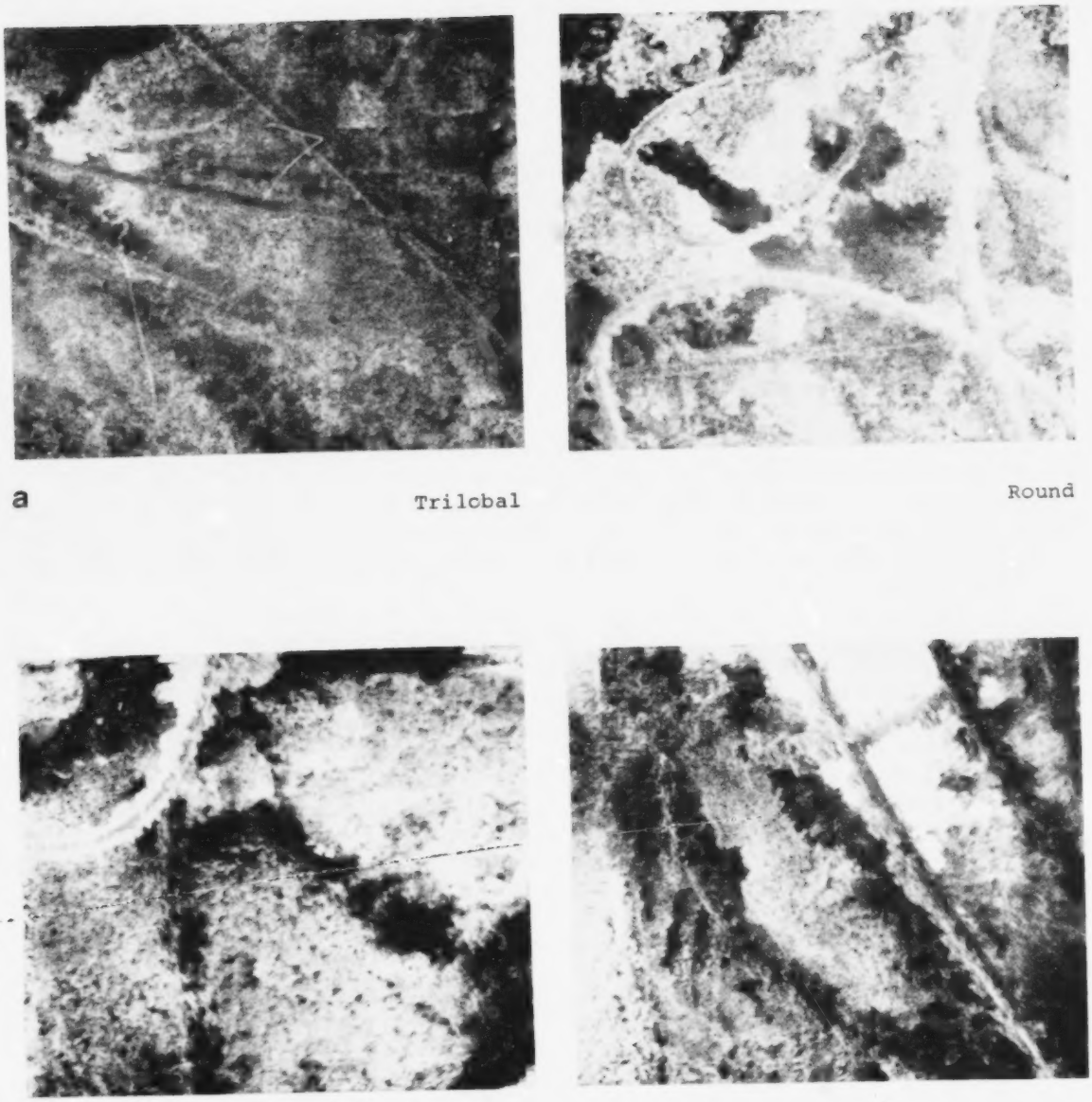

Figure 8. Scanning electron micrographs comparing dust cakes formed on (a) trilobal and round fiber filters (200X), and (b) rough and smooth fiber filters (100X) by a neutralized flyash aerosol.

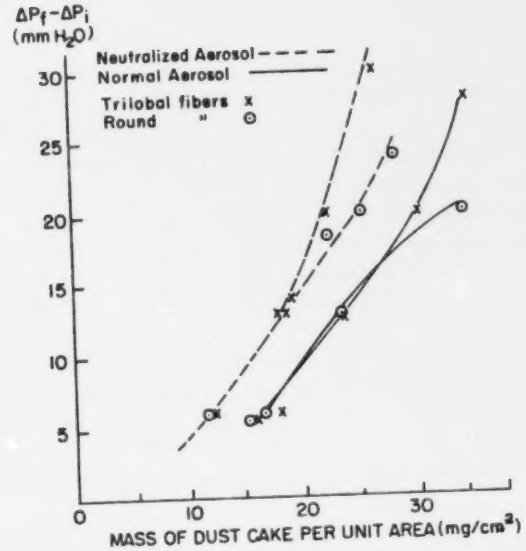

Figure 9. Pressure drop developed by increasing dust cake deposits of untreated and neutralized flyash aerosols on trilobal and round fiber filters.

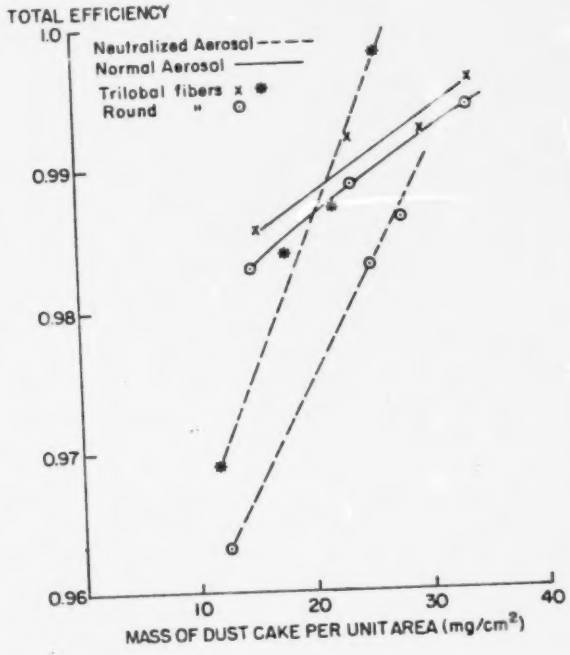

Figure 10. Efficiency of trilobal and round fiber filters with increasing deposits of untreated and neutralized flyash.

compact, less porous cakes. The point at which the "trilobal" pressure drop curve begins to climb above the "round" curve is at a lower cake mass (18 mg/cm^2) for flyash passed through the neutralizer. This is still higher than normal operating cake mass. Baghouse comparisons have verified that trilobal fiber filters do not develop higher pressure drops than round fiber filters up to dust loadings of 24 mg/cm^2 [1,2]. Therefore, these patch-filter data put a practical limit on the finding that trilobal fiber filters are not detrimental to pressure drop even though interfiber spacings are smaller.

The data in Figure 10 show that trilobal fiber filters are more efficient than round fiber filters, even in this high cake mass region. For particles passed through the neutralizer, the effect of cake mass on capture efficiency is more acute, since both lines rise quite rapidly from lower efficiency values at low cake mass.

In Figure 11 it is seen that pressure drops for rough and smooth fiber filters behave similarly as a function of cake mass for both neutralized and unneutralized particles, even at high cake mass. Once again neutralized particles produce cakes with higher pressure drop. In Figure 12 no clear difference in capture efficiency between rough and smooth fiber filters can be seen at any cake mass or for either aerosol. These findings verify earlier results for overall efficiency. The previously observed tendency for conditioned rough fiber filters to capture more submicron particles than smooth ones and the dependence of this tendency on particle charge remain subjects for further study.

2. Effect of Particle Precharging

A final trial with needled filters involved the deposition of extra charges on the aerosol particles. A 15-cm long, 3-cm diameter corona discharge tube was made with a 45-μm diameter axial wire and grounded wall. The aerosol was passed through the tube before proceeding to the duct upstream of the patch filter. With an applied voltage of 10 kV a purple glow could be seen near the wire, and when the flyash aerosol was passed through the tube it was found that no dust emerged from the downstream end, all of it having been deposited in the tube by electrostatic precipitation. The voltage was therefore reduced to the point where some dust could be seen to emerge from the tube, even though at this level there was no visible discharge and no detectable current. Filtration performance of trilobal and round fiber fabrics for this aerosol were compared, and the results are given in Table 2 together with those for a neutralized flyash. For both trilobal and round fibers, efficiency increases and specific cake resistance decreases as the particle charge increases. This gives evidence of the strong influence of coulombic forces. The actual charges on the particles could not be measured at this time. The ability to measure particle-charge distribution would, however, be an asset in the quantitative interpretation of electric phenomena in fabric filtration, and efforts will be made to secure appropriate instrumentation.

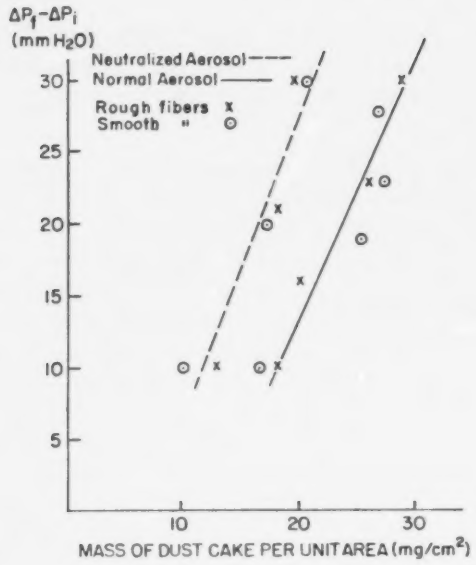

Figure 11. Pressure drop developed by increasing dust cake deposits of untreated and neutralized flyash aerosols on rough and smooth fiber filters.

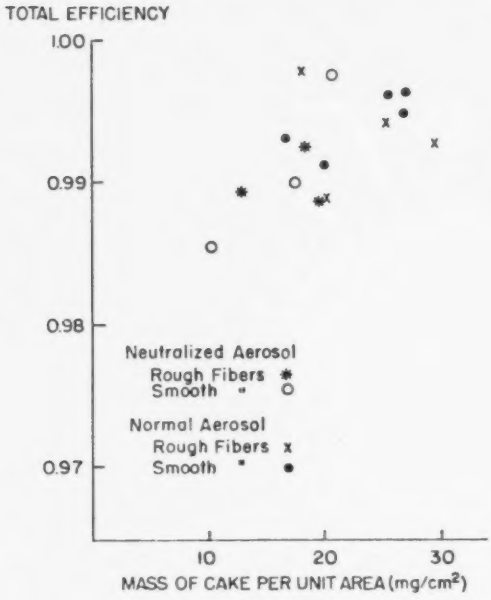

Figure 12. Efficiency of rough and smooth surface fiber filters with increasing deposits of untreated and neutralized flyash.

TABLE 2. CAKE RESISTANCE AND EFFICIENCY OF ROUND AND TRILOBAL FIBER FILTERS WHEN FILTERING AEROSOLS CHARGED TO VARIOUS LEVELS

	Round		Trilobal	
	(10^4 N·s/kg·m)	E(%)	(10^4 N·s/kg·m)	E(%)
Neutralized	1.20	98.30	1.17	98.44
As is	0.60	99.69	0.55	99.86
Charged (5 kV)	0.47	99.88	0.47	99.94

SECTION III

STUDIES OF CAPTURE IN ELECTRIC FIELDS

A. THEORETICAL STUDIES

1. Effect of Field Orientation

The following section gives an account of computer studies on the capture efficiency of single fibers and mats in the presence of electric fields. Several subjects are dealt with. The first concerns the orientation of the electric field with respect to the flow direction and the fiber axis. In 1965, Zebel [2] set forth a theory to account for the effect of an electric field in the capture of particles on cylindrical fibers. Since he envisioned practical applications that would use an electric field parallel to the flow direction, he did not consider the effects of field orientation. What follows is an extension of Zebel's theory to perpendicular fields.

The cases of charged and uncharged particles must be considered separately. Taking first the case of uncharged particles that are acted on by polarization forces caused by the electric field in the presence of a fiber, we note that Zebel showed the collection efficiency for such uncharged particles to depend on two dimensionless parameters, F and a. The latter can have values between 0 and 1, with 0.5 being a typical value. F depends on: the radius of the fiber r_c, the particle radius r_s, the field strength E_o, the gas flow velocity V_o, the gas viscosity μ, and the dielectric constants of the fiber and the particle, σ_c and σ_s, respectively. F is given by

$$F = \frac{4}{3} \left(\frac{\sigma_s - 1}{\sigma_s + 2}\right) \left(\frac{\sigma_c - 1}{\sigma_c + 1}\right) \frac{r_s^2}{r_c} \frac{E_o^2}{\mu V_o} .$$

For field strengths of 2 kV/cm and gas velocities of about 12 fpm, F will vary typically between 10^{-3} and 1.0.

For this problem, Zebel's equations do not have an analytical solution, so that the collection efficiencies were determined by numerically integrating the particle trajectory equations.

Table 3 presents values of the collection efficiency for several values of F; $\eta_{||}$ denotes the efficiency when the field is parallel to the flow, and $\eta_{\perp}$ when the electric field is perpendicular. The collection efficiency is defined as the thickness of the layer in the undisturbed flow (H in Fig. 13) in front of the fiber from which all aerosol particles are captured, divided by the fiber diameter $2 r_c$. We note from Table 3 that over the range of values of F that were studied, a field that is perpendicular to the flow direction yields a higher collection efficiency in every case.

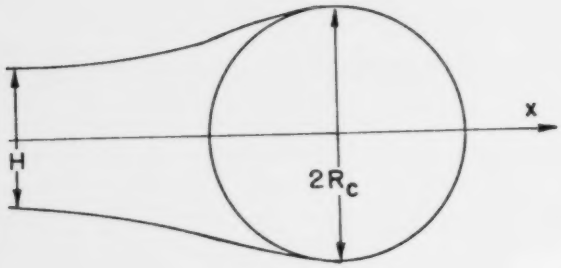

Figure 13. The two limiting particle trajectories for a round fiber of radius r_c.

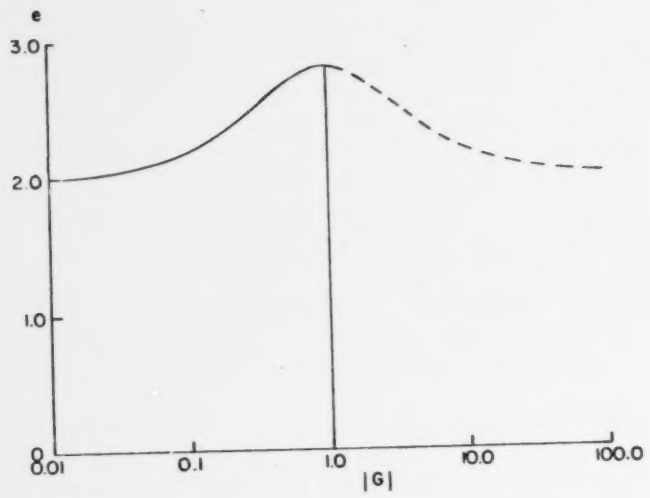

Figure 14. Enhancement e of collection efficiency by a field perpendicular to the flow for charged particles as a function of $|G| = qE_0B/V_0$.

TABLE 3. COMPARISON OF COLLECTION EFFICIENCIES FOR UNCHARGED PARTICLES ACTED ON BY ELECTRIC FIELDS PARALLEL AND PERPENDICULAR TO THE FLOW DIRECTION

F	$\eta\|\|$	$\eta\perp$	Improvement of $\eta\perp$ over $\eta\|\|$ (%)
3.2	1.386	1.517	9.5
1.0	0.630	0.778	23.5
0.5	0.390	0.477	22.5
0.2	0.206	0.240	16.5
0.1	0.115	0.136	18.3
0.02	0.0295	0.0337	14.2
0.01	0.0127	0.0164	29.1

We now consider the collection of charged particles on cylindrical fibers. Zebel showed that in the case where the electric field is parallel to the flow, the collection efficiency is given as:

$$\eta|| = o \quad \text{for } -1<G\leq o, \quad \text{(negative particles)}$$

$$\eta|| = \frac{G(1+a)}{G+1} \quad \text{for } G\geq o, \quad \text{(positive particles)}$$

where $G = E_o q/6\pi\, r_s\, V_o$, and q is the amount of charge on the aerosol particle. Typical values of G for E_o = 2 kV/cm and V_o = 12 fpm are usually between 10^{-3} and 1.0. Since, when G<-1, the particle will move away from the filter against the gas flow, this region is not considered. Zebel did not consider the case where the charged particles are influenced by a field that is perpendicular to the flow, so we have derived the following equation for this case:

$$\eta\perp = \frac{G(1+a)}{(G^2+1)^{\frac{1}{2}}} \ .$$

We can now calculate the enhancement of the collection efficiency due to the use of the perpendicular field to be:

$$\frac{\eta\perp}{\eta||} = \frac{2(G+1)}{(G^2+1)^{\frac{1}{2}}} \ ,$$

if we assume the aerosol to have an equal number of positively and negatively charged particles. The graph of this function over five orders of magnitude for |G| is shown in Figure 14. The broken portion of the curve applies only to positive values of G, corresponding to positively charged particles. For values of |G| less than 0.01 there is no benefit in using the perpendicular field configuration. The maximum benefit is obtained at |G| = 1.0, when the improvement is equal to $2\sqrt{2}$. We conclude, therefore, that for values of F and G

typically met in experimental work the preferred orientation of the electric field is perpendicular to the flow direction.

2. Fibers With Lobed Cross Sections

A second question that was attacked was that of the effect of fiber cross-sectional shape on capture efficiency when electric fields are present. Round and multilobal shapes were considered.

In cylindrical polar coordinates (ρ,ϕ) the equation that describes the boundary of a cylindrical fiber is $\rho=1$. Multilobal fibers are appropriately described by the equation

$$\rho = 1 + \varepsilon \cos m(\phi+c) ,$$

where m is the number of fiber lobes, c is a phase angle that determines the orientation of the fiber to the flow, and ε is a parameter that determines the size of the lobes and is never greater than 1.0.

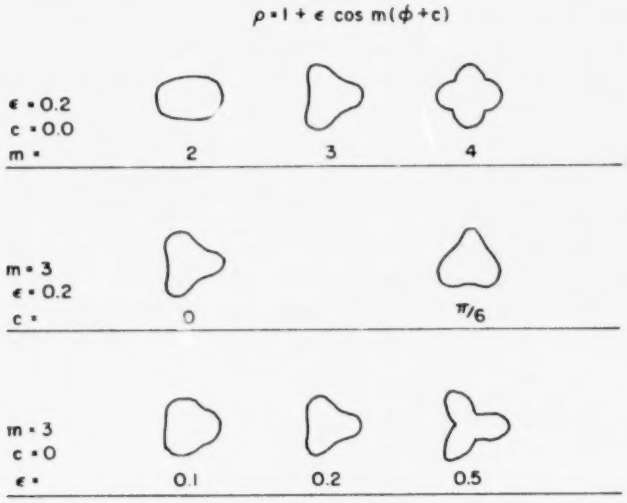

Figure 15. Fiber cross sections for selected values of m (number of fiber lobes), c (orientation of fiber to air flow), and ε (size of lobes).

Figure 15 shows how the cross sections vary for different values of these parameters. The equation for the surface of the fiber suggests that it may be possible to solve for the velocity and electrical force fields as regular perturbation series in the parameter α. We have obtained these solutions and have subsequently solved the trajectory equations for multilobal fibers. Figures 16 and 17 indicate these trajectories for bilobal and trilobal fibers.

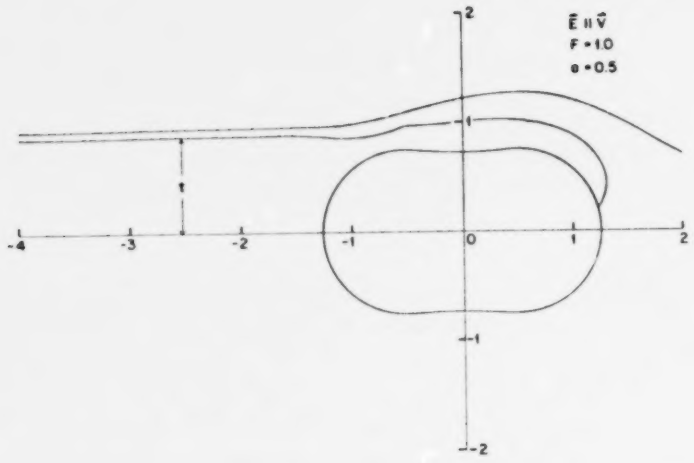

Figure 16. Particle trajectories near a bilobal fiber. Field parallel to air flow, $\alpha = 0.5$, and $F = 1.0$. All particles within the region 2t will be captured.

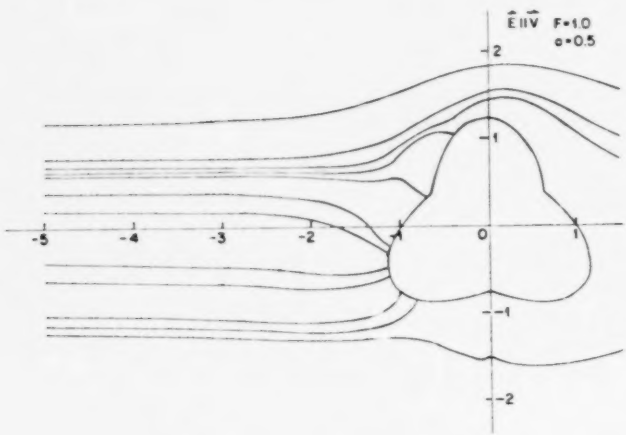

Figure 17. Particle trajectories near a trilobal fiber. Field parallel to air flow, $\alpha = 0.5$, and $F = 1.0$.

Since these fiber cross sections are not symmetric with respect to the flow, the collection efficiencies must be averaged over all possible orientations. Figure 18 shows the collection efficiencies (evaluated for F = 1.0) for a trilobal and a bilobal fiber in an uncharged-particle aerosol. Because of the symmetry of the problem, only values of c between zero and π/m need be considered. Shown at the bottom of Figure 18 are the orientations of the fibers for which the collection efficiencies were calculated. The dotted lines are the values of the collection efficiencies averaged over all orientations of the fibers.

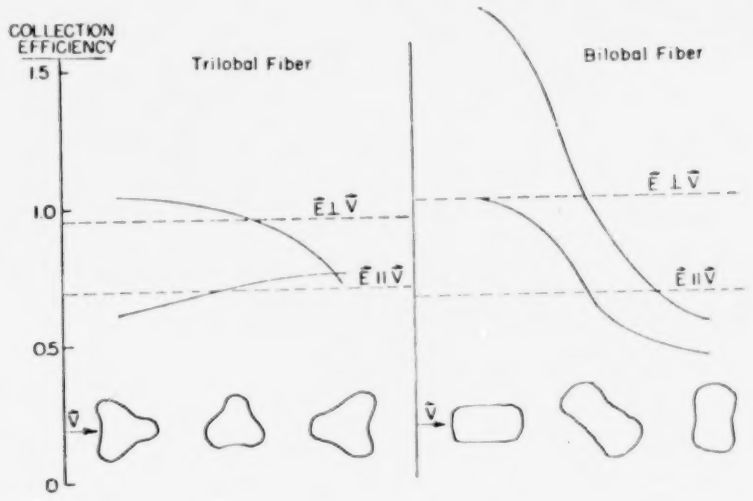

Figure 18. Comparison of collection efficiencies for bilobal and trilobal fibers at different orientations of fiber to electric field.

Table 4 compares the average collection efficiencies of circular, bilobal, and trilobal fibers for F = 1.0. The results indicate that when the electric field is perpendicular to the fiber and to the gas flow, the collection efficiency is greater than when the field is parallel to the gas flow direction.

TABLE 4. COLLECTION EFFICIENCIES FOR UNCHARGED PARTICLES ON 1-,2-, AND 3-LOBE FIBERS IN ELECTRIC FIELDS

Fiber cross section	E||V	E⊥V	Improvement of ⊥ over || (%)
Cylindrical	0.630	0.778	23.5
Bilobal	0.668	1.015	51.9
Trilobal	0.697	0.953	36.7

To calculate the effects on the capture of charged particles we consider the effective diameter of the fiber. Figure 13 illustrates the two limiting trajectories for a round fiber. The effective fiber diameter H is defined to be the distance, measured far upstream from the fiber, between the two limiting trajectories. The single-fiber collection efficiency is then defined as the effective fiber diameter divided by the projected area per unit length of fiber; for the circular fiber shown above this would be $H/2r_c$, where r_c is the fiber radius.

A criterion is now determined on which the capture of particles on multilobal fibers can be compared. Multilobal fibers can have much larger effective diameters than circular fibers, but, since they can have larger projected area, the effect on the collection efficiency will be less pronounced than the effect on the effective diameter.

The single-fiber effective diameter can be related to the collection efficiency of the fiber mat ζ by considering a mass balance on a differential element of the mat. The cross-sectional area of a multilobal fiber is $\pi r_c^2(1+\frac{1}{2}\varepsilon^2)$, or πr_c^2 for round fibers where $\varepsilon=0$. If we define l_f as the length of fiber in a unit volume of mat, then the volume fraction of fibers $\bar{\alpha}$ is given by

$$\bar{\alpha} = \pi r_c^2 \, l_f \, (1+\tfrac{1}{2}\varepsilon^2) \quad .$$

If Q is the flow rate of air into the mat, we expect the air velocity inside the mat V to be

$$V = \frac{Q}{A(1-\bar{\alpha})} \, ,$$

where A is the area of the mat perpendicular to the flow. This velocity is greater than the velocity of air which approaches the mat, since the portion of space in the mat available to accommodate the air is $(1-\bar{\alpha})$.

Consider now a differential element whose thickness is ΔZ and whose area is A. For an aerosol of concentration C, the flow rate of aerosol into this element is CQ, and the flow out is $(C+\Delta C)Q$. The total length of fiber in this element is $A\Delta Z\, l_f$; therefore the amount of aerosol that gets captured on these fibers is $CVHl_fA\Delta Z$. A mass balance on the aerosol yields

$$\underset{\text{(Aerosol In)}}{CQ} - \underset{\text{(Aerosol Out)}}{(C+\Delta C)Q} = \underset{\text{(Aerosol Captured)}}{CVHl_fA\Delta Z} \quad .$$

Substituting for l_f and letting ΔZ, $\Delta C \longrightarrow 0$ yields

$$\frac{dC}{C} = \frac{-H\bar{\alpha}}{(1+\frac{1}{2}\varepsilon^2)\pi r_c^2(1-\bar{\alpha})} \, dZ$$

Let C_o be the aerosol concentration entering the mat and C_f the concentration leaving it. The integration of the above equation yields

$$\frac{C_f}{C_o} = e^{-\gamma} ,$$

where $\gamma = \frac{H\bar{\alpha}L}{\pi r_c^{\,2}(1+\frac{1}{2}\varepsilon^2)}$ and L is the mat thickness. The overall mat collection efficiency is then

$$\zeta = 1 - \frac{C_f}{C_o} = 1 - e^{-\gamma} .$$

Later results may be more easily appreciated after a simple calculation to demonstrate the importance of γ. Suppose that a mat has a collection efficiency of 0.900 when $\gamma = \gamma_o$. If, by changing the field-flow orientation or by adding fiber lobes, γ can be increased by 50%, ζ becomes 0.965; for a 100% increase in γ, ζ=0.990. Since we wish to compare ζ for mats of equal volume fraction and thickness, the best way to compare the collection performance of multilobal fibers is then to compare values of $H/(1+\frac{1}{2}\varepsilon^2)$.

It has been shown that the effective fiber diameter for the collection of charged particles on single fibers is

$$H_1 = 2\left(\frac{G}{G+1}\right) Z(a,\varepsilon,m) ,$$

when the field and flow are parallel, and

$$H_2 = 2\left(\frac{G}{\sqrt{G^2+1}}\right) Z(a,\varepsilon,m) ,$$

where the field is perpendicular to the flow. The quantity Z is a function of only fiber geometry and a, where

$$a = \frac{\sigma_c - 1}{\sigma_c + 1} .$$

These values of H are the effective fiber diameter averaged over all fiber orientations ($0 \le c \le \pi/m$).

As in the case of round fibers, we see that the perpendicular electric field case provides an enhancement of $e = \frac{G+1}{\sqrt{G^2+1}}$ when all

the particles are positively charged, and $e = \frac{2(G+1)}{\sqrt{G^2+1}}$ when there are equal numbers of positively and negatively charged particles. The enhancement due to the field orientation is therefore independent of fiber geometry.

It can be shown that for a circular fiber $Z = 1 + a$; therefore the largest value of Z occurs at $a = 1$. Since Z is expected to be a maximum at $a = 1$ for multilobal fibers, and since the attempt here was to investigate the extent to which multilobal fibers provide an enhancement of the fiber mat collection efficiency, we confine our attention to the case where $a = 1$.

As discussed earlier, the appropriate parameter for comparing multilobal and circular fibers is $H/(1+\frac{1}{2}\varepsilon^2)$. Since Z does not depend on the field-flow orientation and therefore isolates the effects of a, ε, and m, then $Z/(1+\frac{1}{2}\varepsilon^2)$ can be seen to provide the most useful index for evaluating the effect of fiber geometry on the fiber mat collection efficiency. Since the value of $Z/(1+\frac{1}{2}\varepsilon^2)$ is $(1+a)$ for cylindrical fibers, the enhancement over cylindrical shape provided by a multilobal shape will be given by $Z[(1+a)(1+\frac{1}{2}\varepsilon^2)]$ or, for $a = 1$, $Z/(2+\varepsilon^2)$.

Figure 19 shows a plot of this latter parameter vs. ε for various multilobal fibers; the integers on each curve are the values of m along that curve. This figure indicates that for commercially available bilobal and trilobal fibers (where $\varepsilon \gtrsim 0.3$) enhancements of up to 50% can be expected. Figure 20 attempts to portray the levelling out of this enhancement with m. We can extrapolate these curves to estimate the effect of fiber surface roughness for which, say, $\varepsilon = 0.01$ and $m = 100$. The extrapolated value of the enhancement would be approximately 3-4%, thus, causing a very small effect on the fiber mat collection efficiency.

Figure 19 suggests that fiber lobes will always enhance the collection efficiency. This statement is true except for the case of bilobal fibers for which the enhancement strongly depends on the orientation of the fiber to the air flow. Figure 21 illustrates the wide range of enhancements that are possible with bilobal fibers. The effect is greatest when the major axis of the fiber is perpendicular to the flow ($2c/\pi = 0.5$). When the fiber lies flat and the lobes are aligned with the flow, the collection efficiency is less than that for round fibers. For trilobal and other multilobal fibers this orientation dependence is not important. Therefore our results suggest that, except for bilobal fibers, fiber lobes will always enhance the collection of charged particles and that this effect levels off after about five lobes.

The above calculations indicate that in the presence of electric fields, rough or lobed fibers produce greater collection efficiencies than smooth or round fibers. This may provide a partial explanation for the better performance of mats of lobed fibers. If the aerosol contains charged particles, their deposition will set up electric fields near the upstream fabric surface. In the presence of these

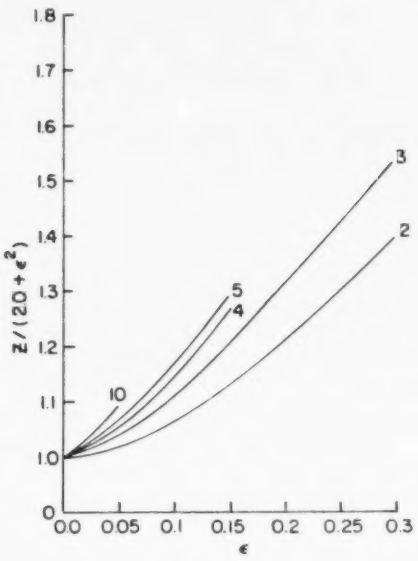

Figure 19. Comparison of the effective diameters of multilobal fibers (for charged particles). Number of lobes indicated on curves; ε indicates depth of lobes.

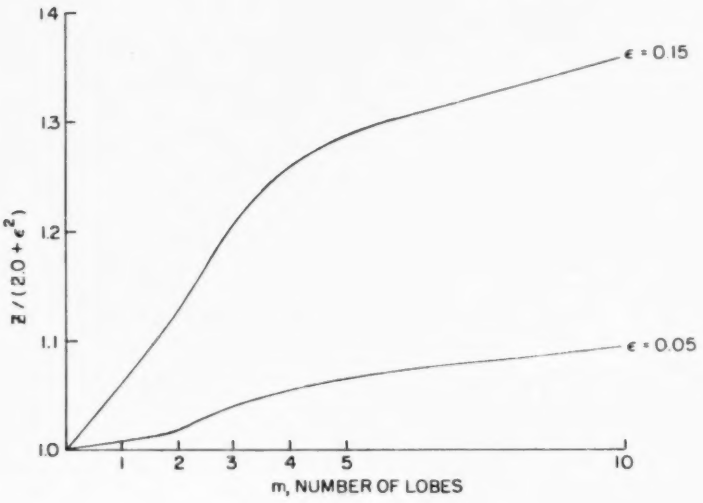

Figure 20. Effective fiber diameter vs. number of lobes (for charged particles).

fields, capture of subsequent particles will be more efficient on lobed fibers. This hypothesis will be tested in a future grant period.

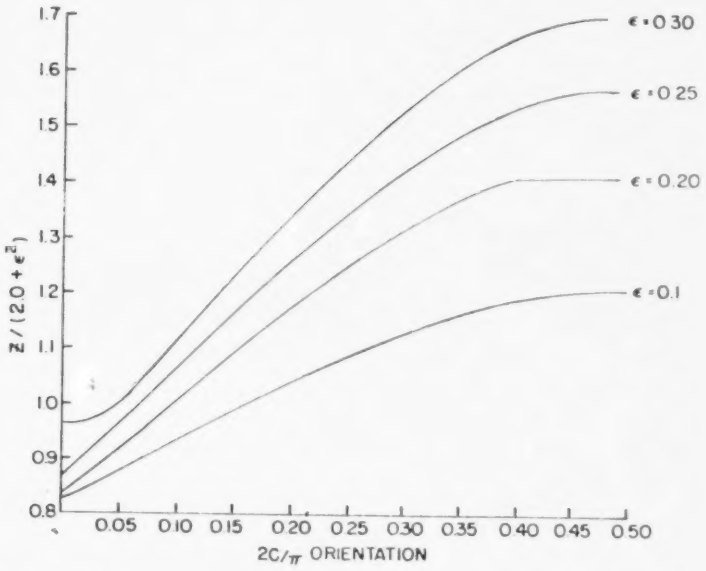

Figure 21. Effect of fiber orientation on the effective diameter of a bilobal fiber (for charged particles).

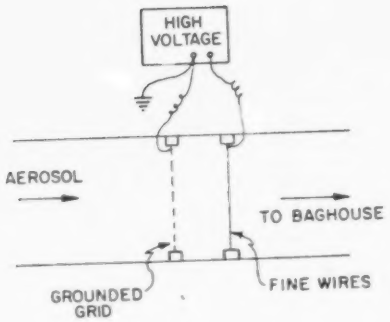

Figure 22. Diagram of tube for precharging flyash aerosol (negative precharging arrangement).

B. EFFECT OF ELECTRIC FIELD ON CAKE STRUCTURE

1. Introduction

Applying a high voltage across wire electrodes embedded 15 mm apart just below the filter surface has produced not only higher filtration efficiencies but also lower pressure drops. The increase in efficiency is considered to be a result of the deflection of particles from the normal air stream under the influence of the electric field. This increases the probability of impact with a fiber or a particle of dust in the dust cake. Consequently, a lower concentration of particles passes through the filter. If incoming particles are already charged naturally or by corona precharge, they will drift in the direction of the electrode of opposite charge. If incoming particles are neutral, they may be influenced by polarization forces acting in the non-uniform field in the neighborhood of a fiber. Rivers [3] considered the two mechanisms of coulombic and polarization forces and raised the question of whether coulombic forces alone may not account for observed efficiency improvement.

The decrease in pressure drop under the influence of the electric field is more difficult to explain and is the main subject of this study. The lower pressure drop is most likely due to a different cake structure. Because of the magnitude of the effect, differences in cake structure should be detectable.

2. Experimental Results

Flyash cakes formed under the influence of an electric field on patch filters with wire electrodes embedded below the upstream fabric surface were examined in a binocular microscope. Incoming particles were used as they were from the feeder, or else they were passed through a precharging tube or through a neutralizer. The precharging tube is shown in Figure 22. It contains an open wire mesh electrode located upstream from a series of fine wires as the other electrode. The neutralizer is a tube containing a radioactive source (krypton 85). The experimental design was as follows:

Trial No.	Precharge voltage (kV)	Positive downstream	Negative downstream	Potential gradient across filter (kV/cm)
1	11	X		0
2	11	X		2
3	11		X	2
4	14	X		2
5	14		X	2
6	Particles through neutralizer			0
7	Particles through neutralizer			2
8	Untreated particles from feeder			0
9	Untreated particles from feeder			2
10	Two isolated electrodes-particles from feeder			2

The following observations are illustrated in the photographs of Figures 23-30:

1) No field across filter

If a potential gradient is not applied to the filter (Trial nos. 1, 6, and 8, Figs. 23-25), the cake deposits uniformly over the filtering surface. Neutralized particles (Fig. 24) appear slightly more densely packed than charged particles (Figs. 23 and 25), which apparently have a tendency to collect closer to the surface and do not collapse into pores as readily. These observations agree with previous pressure drop measurements in which the highest value was obtained for neutralized particles and the lowest values for charged particles.

2) Potential gradient applied across filter - 2 kV/cm

When a potential gradient of 2 kV/cm is applied across the filter, the cake no longer deposits uniformly over the filtering surface. Using untreated particles (Trial no. 9, Fig. 26), the amount of dust is greater on the negative electrodes with particles depositing on fibers raised above the surface. The positive electrodes are covered by dust but deposition is lower. If particles are precharged positively (Trial no. 2, Fig. 27), cake formation is similar to that of Trial no. 9. The implication is that untreated dust from the feeder is predominantly positively charged, so that it behaves like the positively precharged dust and deposits mainly on the negative electrodes of the filter.

If the precharge is then reversed so as to charge the particles negatively (Trial no. 3, Fig. 28), the deposition becomes equal on all wires. Reversing the charge apparently does not change all the original positive charges to negative but does change enough of them so that deposition is about equal. Increasing precharge voltage (Trial nos. 4 and 5) had no observable effect.

If the particles are passed through a neutralizer (Trial no. 7, Fig. 29), there is still a greater deposition of particles on the negative electrodes in the filter, but the difference is not as pronounced. Apparently not all particles are neutralized, and some positively charged particles still remain in the aerosol.

These observations clearly support the dominance of the coulombic force in the electrical stimulation of fabric filtration (ESFF). If polarization forces were dominant, the distribution of dust would be equal on all electrodes. The preferential deposition over certain electrodes in all these cases is more easily explained by the coulombic mechanism.

3) Isolated pairs of electrodes - 2 kV/cm

In another experiment two electrodes 10 mil in diameter were embedded on one half of the filter and two electrodes 2 mil in diameter were embedded on the other half. Any differences in pattern

Figure 23. Positively precharged particles deposited on filter in absence of applied field across filter.

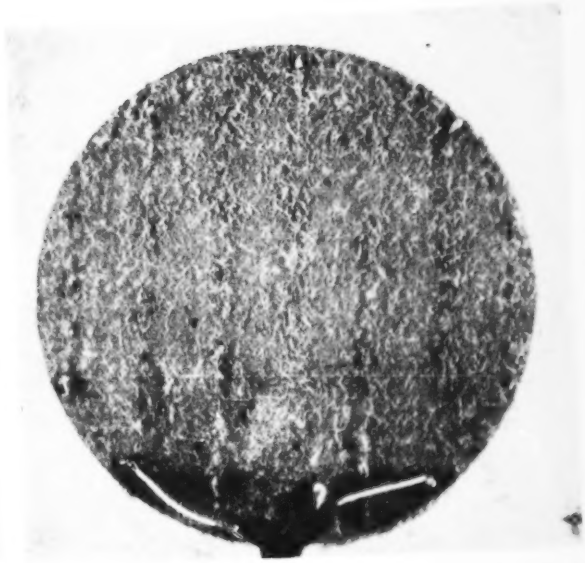

Figure 24. Neutralized particles deposited on filter in absence of applied field across filter.

Figure 25. Naturally charged particles deposited on filter in absence of applied field across filter.

Figure 26. Naturally charged particles deposited on filter with 2 kV/cm across filter.

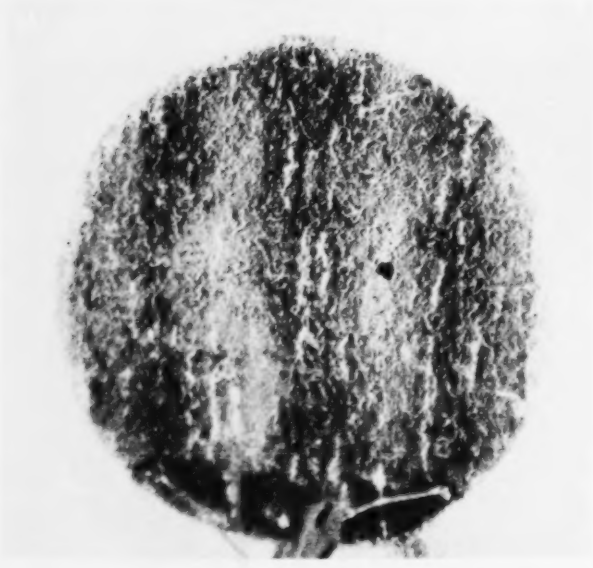

Figure 27. Positively precharged particles deposited on filter with 2 kV/cm across filter.

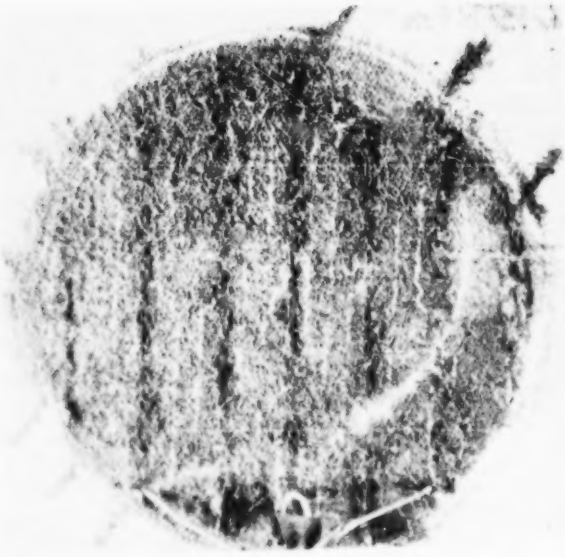

Figure 28. Negatively precharged particles deposited on filter with 2 kV/cm across filter.

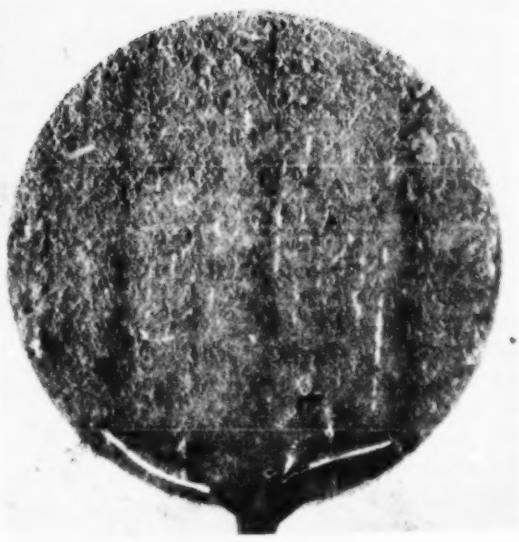

Figure 29. Neutralized particles deposited on filter with 2 kV/cm across filter.

Figure 30. Two sets of two electrodes with 2-kV/cm potential gradient using naturally charged particles. (Left side: + -, 10 mil diam. Right side: - +, 2 mil diam.)

due to wire diameter are too slight to be noticed at 2 kV/cm using naturally charged particles (Fig. 30). However, this sample filter provides further clues to the mechanism of deposition in an electric field. In the central region of the filter, there is no field since the central electrodes (2 mils and 10 mils) are both negative. Greater penetration into the filter occurs in this region as compared to the regions between electrodes where dust is closer to the surface.

If only two wires are embedded in the filter surface and one has a potential of 2 kV/cm, incoming untreated particles will deposit over the negative wire but will leave the positive wire clean. With alternating wires (Trial no. 9, Fig. 26), the positive wires received some deposit. Apparently, the deposition on the positive wires in the alternating wire arrangement is due to direct impingement in the region near the positive wire where the field force drawing particles to the adjacent negative wires is balanced. This effect would support the supposition that particles coming directly from the feeder are mostly positive. Measurement of actual particle charge should be performed to verify this hypothesis. Similar measurements should also be made on particles passed through the corona and through the neutralizer.

The observation that in the presence of electric fields dust deposition is not uniform offers a possible mechanism to explain reductions in pressure drop. Uneven dust deposition would create filter regions with paths of different resistance to air flow. Resorting to an electrical analogy, we note that the effective resistance of two parallel resistors is highest when their resistances are equal. Figure 31 plots the effective resistance of two such resistors as their values are unbalanced, while the sum of their resistances remains constant, just as the total mass of dust reaching the filter remains constant. It is seen that for this model a resistance inbalance of about 6 to 1 cuts the pressure drop (effective resistance) in half.

3. Conclusions

Two mechanisms appear to act in reducing resistance to air flow through a dust cake formed under the influence of an electric field. The first is the tendency for particles to deposit closer to the surface and not to collapse into the pores, thereby producing a cake with a lower packing density. This effect occurs for charged particles even in the absence of an electric field. The second mechanism is the uneven distribution of dust on electrodes due to the coulombic attraction of charged particles to the oppositely charged electrode. The more uneven the distribution the lower will be the resistance to air flow. The two mechanisms combined produce a cake having much lower specific resistance than one formed in the absence of potential gradients.

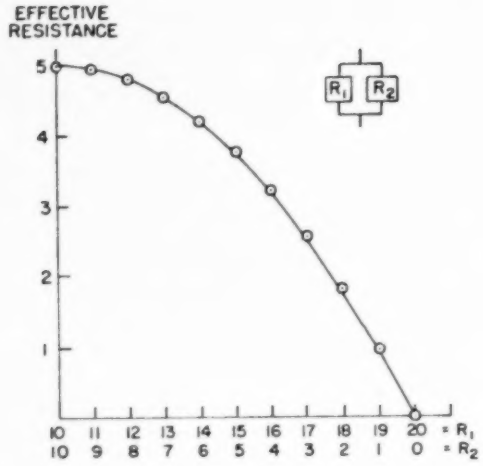

Figure 31. Electrical analogy of unequal parallel resistances.

SECTION IV

REFERENCES

1. Miller, B., G. Lamb, P. Costanza, and J. Craig, "Nonwoven Fabric Filters for Particulate Removal in the Respirable Dust Range," EPA-600/7-77-115, U. S. Environmental Protection Agency, October 1977.

2. Zebel, G., Deposition of Aerosol Flowing Past a Cylindrical Fiber in a Uniform Electric Field, J. Colloid. Sci. 20, 522-543 (1965).

3. Rivers, R. D., "Operating Principles of Non-Ionizing Air Filters," ASHRAE Journal, February 1962.